



ISSN: 2230-9926

Available online at <http://www.journalijdr.com>

IJDR

International Journal of Development Research

Vol. 13, Issue, 06, pp. 62946-62951, June, 2023

<https://doi.org/10.37118/ijdr.26836.06.2023>



RESEARCH ARTICLE

OPEN ACCESS

EVALUATION OF THE ACTION AND PROPERTIES OF THERMOPLASTIC STARCH / TITANIUM DIOXIDE / GRAPHENE NANOCOMPOSITES OBTAINED THROUGH SPRAY DRYING FOR FRUIT COVERING

Thaís Guimarães Guerra, Renata da Silva Cardoso, Gisele Cristina Valle Iulianelli, Paulo Sergio Rangel Cruz da Silva and Maria Inês Bruno Tavares*

Instituto de Macromoléculas Professora Eloisa Mano, Universidade Federal do Rio de Janeiro, RJ, Brasil Cidade Universitária – Centro de Tecnologia – Bloco J, CEP: 21945-970 – Rio de Janeiro, Brasil

ARTICLE INFO

Article History:

Received 14th April, 2023

Received in revised form

26th April, 2023

Accepted 20th May, 2023

Published online 30th June, 2023

KeyWords:

Nanocomposites, Starch, Titanium Dioxide, Graphene, Biodegradable Polymer.

*Corresponding author:

Maria Inês Bruno Tavares

ABSTRACT

In this study, nanoparticles of titanium dioxide (TiO₂) and graphene were incorporated into a matrix of thermoplastic starch (TPS) obtained from cassava (*Manihot esculenta* Crantz) with the objective of producing a material for covering fruit, aiming to last the shelf life of food. The polymeric nanocomposites (NCPs) were obtained by the solvent dispersion method and, subsequently, the spray drying technique was used to obtain the material in powder form. The NCPs were characterized by Fourier transform infrared spectroscopy (FTIR), X-ray diffraction (XRD), fluidity index (MFI), dynamic light scattering (DLS), zeta potential (PZ) and UV absorption spectroscopy ultraviolet and visible (UV-vis). The main results showed that the polymeric suspension obtained from the pulverized nanocomposites presented characteristics for potential use in coating apples and guava, such as high efficiency in absorbing UV-A and UV-B radiation and high stability of the formed solutions. Furthermore, the fruit coating test proved that the developed solution improved the visual characteristics and significantly delayed the degradation process of the analyzed fruits, proving to be effective in offering greater longevity to the food, reducing exorbitant losses and waste that strongly impact positively the economy and the environment.

Copyright©2023, Thaís Guimarães Guerra et al. This is an open access article distributed under the Creative Commons Attribution License, which permits unrestricted use, distribution, and reproduction in any medium, provided the original work is properly cited.

Citation: Thaís Guimarães Guerra, Renata da Silva Cardoso, Gisele Cristina Valle Iulianelli et al., 2023. "Evaluation of the action and properties of thermoplastic starch/titanium dioxide/graphene nanocomposites obtained through spray drying for fruit covering". *International Journal of Development Research*, 13, (06), 62946-62951.

INTRODUCTION

Food losses and waste occur along the entire agricultural value chain and at all stages of production until it reaches the consumer's table. The most recent data released by the UN, in the 2021 food waste index report, reveal that about 931 million tons of food were lost and wasted in the world in 2019, equivalent to 17% of all food produced for human consumption (Forbes, 2021). This number becomes even more impressive when we consider that about a tenth of the world's population, up to 811 million people, went hungry in 2020 (UNICEF 2021). Added to this data, the loss and waste of food also brings disastrous losses generated by the inefficient use of water resources, energy and soil and impacts associated with the deposition of these foods in landfills, which cause pollution and methane production during their decomposition. According to FAO (Food and Agriculture Organization of the United Nations), food loss and waste generate between 8 to 10% of all greenhouse gas emissions produced by humans (FAO, 2019). These data make food loss and waste an important contributor to the three biggest planetary crises: climate

change, loss of nature and biodiversity, and pollution generated by waste (Forbes, 2021). The relevance and urgency of mitigating this damage included this issue as one of the main Sustainable Development Goals (SDGs) at the United Nations General Assembly (UNGA) in 2015. Goal 12.3 sets the objective of halving per capita food waste and losses along the production and supply chains by the year 2030 (IPEA, 2018). Brazil, in particular, presents very worrying data and is among the countries that waste the most food in the world, a profile normally associated with more developed countries (Propino, 2018). According to a study carried out by EMBRAPA, Brazilian families waste, on average, 353 grams of food per day, equivalent to 128.8 kg per year. In per capita analysis, the waste is 114 grams per day, which represents an annual waste of 41.6 kg per person (Propino, 2018). In consequence, in Brazil, there is simultaneously the worrying combination of a high level of food waste with a high number of individuals with food insecurity. According to the Brazilian Research Network on Food and Nutritional Sovereignty and Security (Rede Pennsan), more than half of the Brazilian population (58.7%) lives with food insecurity to some degree, whether mild, moderate or high (Gandra, 2022). As a measure

to reduce all this waste and all associated damage, the United Nations Environment Program (UNEP) and the Food and Agriculture Organization of the United Nations (FAO) carried out in 2021 a digital campaign to raise awareness and actions together with state and municipal governments in various regions of the country (UNEP, 2021). In the field of science, a promising strategy that aims to reduce this waste is the development of coatings for food protection, aiming to extend the shelf life of these products and delay the ripening process. For this purpose, the use of natural and biodegradable polymers is noteworthy. Consequently, in addition, it reduces dependence on polymers of fossil origin and do not run into environmental issues related to the inappropriate disposal of these materials (Shaikh *et al.*, 2021).

Among the natural polymers, starch is highlighted for being an abundant polysaccharide in nature, low cost and widely used. However, despite these advantages, starch has some disadvantages such as low mechanical properties, high hydrophilicity and low dimensional stability when compared to synthetic polymers. In order to overcome these disadvantages, the incorporation of nanoparticles in this polymeric matrix becomes a potential alternative. They make it viable to improve the characteristics of the thermoplastic starch matrix (TPS) and confer new properties with low filler contents (Velasco *et al.* 2021). Films and coatings developed from starch are described as isotropic, odorless, tasteless, colorless, non-toxic and biodegradable (FLORES *et al.*, 2007). In this work, the influence of adding TiO₂ nanoparticles at different concentrations (0.5; 1.0 and 2.0% m/m) and graphene (at a fixed concentration of 0.1% m/m) on the matrix of TPS obtained from cassava, focusing application for edible fruit coatings in order to extend its shelf life, and consequently the waste of food, which rots during its transport to more distant places. Hence, the methodology used to obtain NCPs was the spray drying technique, a viable commercial alternative to obtaining films via casting. This last technique, despite being a very simple and low-cost technique, may have the disadvantages of heterogeneous phases and long drying time. Moreover, the production of nanocomposites by spray drying has the advantages of obtaining directly in powder form; good control of the properties of the powder obtained; production of materials on different scales (laboratory and industrial) and a quick process to obtain the dry material. Hereafter, the product can be solubilized so that it can be used in solution when necessary or used directly for film production. Besides, the spray dryer technique follows the waterless trend, which permits a reduction in packaging consumption and easier transport.

EXPERIMENTAL

Materials: Cassava starch/starch (*Manihot esculenta* Crantz) was supplied by Aminna Alimentos Ltda (moisture content: 7.3%; water solubility index: 47.8% (IWS); anatase titanium dioxide (average diameter of particles of about 25 nanometers) was supplied by Sigma-Aldrich BrasilLtda; the commercial graphene xGnP grade M (average diameter of 5, 15 or 25 microns, depending on the manufacturer, and average thickness of 6-8 nanometers) was supplied by XG Sciences 1 ml/ml glycerol (propane-1,2,3-triol) was supplied by Hemafarma, and anhydrous citric acid was supplied by MV Química Gala apple (*Malus Communis*), green apple (*Malus sylvestris*) and guava (*Psidium guajava*) were supplied by Hortifruti Natural da Terra da Tijuca-RJ.

Preparation of TPS/TiO₂/graphene nanocomposites by spray dryer: Before preparing the solutions, the starch, graphene and titanium dioxide were put in an oven for 40 minutes at 50 °C to remove moisture. Starch solutions in deionized water were prepared at a concentration of 2.5% m/v and glycerol and citric acid were added at 30% and 1%, respectively, in relation to the dry granulated starch mass. Then, 0.5, 1.0 and 2.0% (m/m) of TiO₂ nanoparticles were added and after 2 minutes of stirring, graphene 0.1% (m/m) was added. The formulations were kept under magnetic stirring for 24h. After this step, they were heated at 75 °C for 30 minutes, obtaining complete gelatinization of the starch. The suspensions obtained were subjected to spray drying in the benchtop spray dryer (MSD 0.5 -

Labmaq) under the following conditions: Suspension feed rate 0.20 L; Air inlet temperature in the dryer 100-110 °C; Air outlet temperature in the dryer 90-95 °C; Compressed air pressure 200 KPa; Air flow 2.4 NL/h. The same procedure was performed for the cassava starch solution without the nanoparticles, used as a reference material. Table 1 presents the yield of the material obtained after atomization.

Table 1. Yield of samples of TPS/TiO₂/graphene nanocomposites obtained by spray dryer

Samples	Initialweight (g)	final weight(g)	Percentage (%)
TPS Cassava	5.0	3.03	61%
TPS 0.5% TiO ₂ +0.1% G	5.1	2.52	49%
TPS 1% TiO ₂ +0.1% G	5.1	2.09	41%
TPS 2% TiO ₂ +0.1% G	5.1	2.60	51%

Characterizations

Fourier transform infrared spectroscopy (FTIR): The infrared spectra of the samples were recorded in the FT-IR/FIR Frontier - Perkin-Elmer spectrometer. The spectra were recorded in the range of 4000 to 400 cm⁻¹ with a resolution of 2 cm⁻¹, using 20 scans per spectrum. Samples were prepared using potassium bromide (KBr) pellets.

X-ray diffraction (XRD): The diffractograms of the samples were obtained in a Miniflex, Rigaku diffractometer operated at 30 kV, 15 mA, step of 0.05, sweep rate of 1°/min at room temperature, wavelength of 1,542 Å, corresponding to the CuKα band. The diffraction sweep range was adjusted to angles from 2° to 80° (2θ). The interlamellar distance of the planes was calculated according to the Bragg equation ($2d \sin \theta = n\lambda$). The average size of the crystallites was determined using the Scherrer equation ($D = K\lambda/\beta(\cos \theta)$). The degree of crystallinity X_c (%) of the samples was obtained through the equation ($X_c (\%) = I_c/(I_c + I_a) * 100$) The results were analyzed using the X'Pert High Score Pro software.

Flow index (MFI): The melt index was measured with a 4003 Dynisco capillary tension rheometer according to ASTM D1238 (2020). Temperature used: 190 °C; Warm-up period: 100 seconds; Load: 2.06 Kg; Cuts made: 5; Cutting time: 60 seconds.

Dynamic light scattering (DLS) and zeta potential (ZP): To obtain the DLS and ZP analyses, the Nicomp Nano Z3000 light scattering spectrometer was used. The powdered nanocomposites were previously solubilized in deionized water at a ratio of 1:2 in a quartz cuvette and analyzed in duplicate at a room temperature of 25° C.

Ultraviolet-visible absorption spectroscopy (UV-VIS): The analysis was performed in a BioMate 160 - Thermo Scientific spectrophotometer. The wavelength range used was 190 to 1100 nm, under a scanning range of 1 nm. To calculate the band gap energy, Planck's equation was used ($E = h.c/\lambda$), where: E= Band gap energy; h= Planck's constant: 6.6207.10-34 m².kg/s; c= Speed of light: 299,792,458 m/s; and λ= Wavelength of maximum absorbance.

Coating test: The foods used for the experiment were the Gala apple, green apple and guava provided by local commerce. The suspension selected for coating the fruits had a composition of TPS with 1% TiO₂ and 0.1% graphene. For the Gala apple, the following procedure was performed: Initially, the nanocomposite suspension was gelatinized at 85 °C and after cooling it was sprinkled directly on the surface of the fruit. The apples were hung on the hood railing to spray the solution and kept in a closed hood for observation over 12 weeks. For green apples and guava, an immersion bath was performed with the gelatinized solution at 85 °C. After the solution cooled, the fruit was immersed in it for 5 seconds and then the excess solution was drained into an empty container. Finally, the fruit remained at rest on a support for natural drying and solvent evaporation. Evaporation occurred spontaneously. The fruits remained on the bench at room temperature (30 °C and 70% RH). The control fruits did not receive the coating.

RESULTS AND DISCUSSION

Fourier transform infrared spectroscopy (FTIR): The molecular structure of the starting materials and possible interactions with NPs (TiO_2 and graphene) were evaluated by Fourier transform infrared spectroscopy. Table 2 presents the main cassava starch bands obtained in the FTIR spectrum and their assignments according to literature data.

Table 2. List of the main bands obtained by FTIR and their respective chemical groups

Wave number (cm^{-1})	Assignment	Chemical compound	References
3400	Axial deformation of O-H	Alcohol	ÇIPLAK <i>et al.</i> 2014
2930	Axial deformation of C-H	Alkane	LIM <i>et al.</i> 2018
1645	C-O associated to O-H group	Water	CABELLO-ALVARADO, 2019
1460	Symmetric deformation of CH_2	Alkane	ÇIPLAK <i>et al.</i> 2014
1360	Vibration of O-H	Alcohol	LIM <i>et al.</i> 2018
1157	asymmetric stretch C-O-C	Éter	LIM <i>et al.</i> 2018
1080	Angular deformation C-O	Alcohol primary	ÇIPLAK <i>et al.</i> 2014
1020			LIM <i>et al.</i> 2018
927	α -1,4 C-O-C	Polysaccharide	MIRANDA <i>et al.</i> 2011
860	glicopiranoose C-O-C		LIM <i>et al.</i> 2018
760			

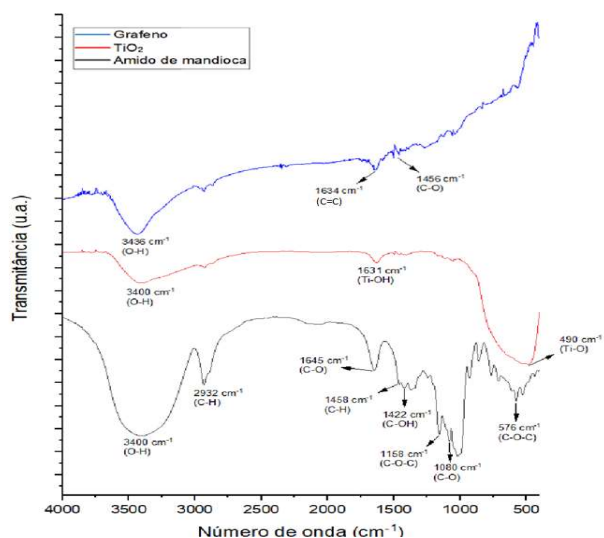


Figure 1. FTIR spectra with the characteristic bands of titanium dioxide, graphene and cassava starch nanoparticles used in this work

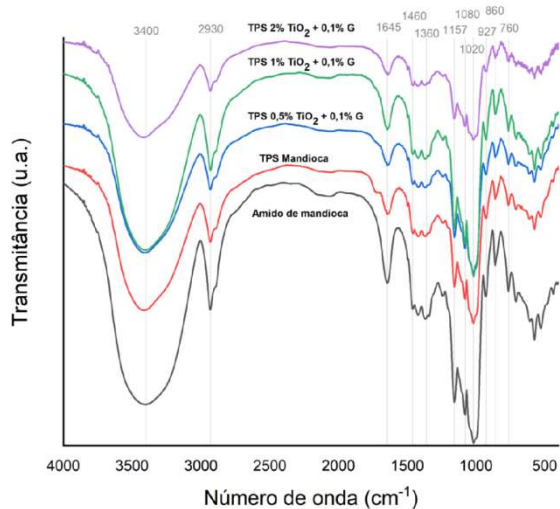


Figure 2. FTIR spectra of mandioca starch, pure TPS and synthesized nanocomposites

From Figure 1, it is possible to observe the absorption band between 3200-3500 cm^{-1} (centered at 3400 cm^{-1}) of starch and glycerol attributed to the stretching vibration of the -OH group due to inter and intramolecular hydrogen bonds. In this absorption range, the characteristic absorption bands of hydroxyl groups adsorbed on the surface of TiO_2 NPs (ZIELINSKA *et al.* 2022) and graphene (ZHU *et al.* 2010) can also be observed. The TiO_2 NPs showed characteristic bands: at 1631 cm^{-1} , corresponding to water-folding in Ti-OH (SIWIŃSKA-CIESIELCZYK *et al.* 2020) and at 490 cm^{-1} , corresponding to the Ti-O-Ti vibration band (CABELLO - ALVARADO, 2019, SIWIŃSKA-CIESIELCZYK *et al.* 2020). For pure graphene, three characteristic bands also stand out: the first at 3436 cm^{-1} is attributed to the stretching vibrations of the -OH groups, the second band at 1456 cm^{-1} corresponds to the -OH deformation (ÇIPLAK *et al.* 2014) and the third characteristic band at 1634 cm^{-1} refers to the C=C elongation (FERREIRA and ANDRADE, 2021). As for nanocomposites, once the NPs are dispersed in the starch matrix, these bands may overlap. However, according to Chen *et al.*, (2019) the addition of NPs and their interaction with the polymeric matrix can promote a decrease in the intensity of the absorption bands, indicating the occurrence of interactions between the materials. This phenomenon was observed in the nanocomposite samples with an increase in TiO_2 concentration, being more clearly evidenced when 2% m/m of this nanoparticle was used, compared to pure TPS (Fig. 2). Considering the chemical structure of the materials used, hydrogen bonds between them are expected. The decrease in absorption intensity observed in the band at 2932 cm^{-1} , corresponding to the C-H bond, can be explained by possible hydrogen bonds between the -CH groups of TPS and the hydroxyls adsorbed on the surface of NPs. Then, such groups would be less available for interaction with infrared radiation. Taking into account nanocomposites, it was not possible to verify characteristic bands of graphene due to overlapping bands or, more likely, due to the low content incorporated in these systems. For the systems containing TPS, the band at 1645 cm^{-1} corresponds to the hydrolysis that occurred between the starch chains with water (Fig. 2). For cassava starch, characteristic absorption peaks are observed in the region between 1656-1640 cm^{-1} associated with the -OH angular curvature of water molecules, while the peak near 2930 cm^{-1} is attributed to the CH vibration and a broad band at around 3400 cm^{-1} is the result of vibration of the hydroxyl group.

X-ray diffraction (XRD): The crystalline profile, size of the crystallites and degree of crystallinity of the systems were evaluated by the X-ray diffraction technique. Figure 3 shows the diffractogram of cassava TPS and its nanocomposites prepared with different amounts of TiO_2 /graphene in the angular range between 2 and 90 2θ degrees.

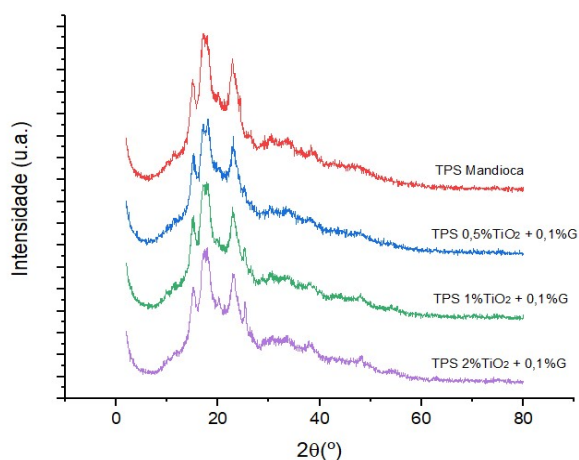


Figure 3. Diffractogram of cassava TPS and nanocomposites obtained

The cassava starch sample exhibited the characteristic peaks of amylopectin at 15.1°, 18.1° and 22.8° (2θ), characteristic of the type C crystalline form (mixed structure type A and B) (HERNANDEZ, 2021; VAN SOEST *et al.*, 1996; THAJAI *et al.*, 2022).

A distinct peak at 9.8° (2θ) is also observed, which can be attributed to variations in the structure of the starch depending on its origin (biological and geographic) or even to the length of the amylopectin chain, amylase and moisture content of the starch from the same original source. In all systems studied, characteristic peaks of the original structure of starch were observed after gelatinization, due to the recrystallization process (OSTAFIŃSKA *et al.*, 2017). With the insertion of TiO_2 NPs in the TPS matrix, the characteristic peak of the anatase phase (plane 101) was observed at an angle of 25.3° (THAMAPHAT *et al.*, 2008, VOEPEL *et al.*, 2018). An increase in the diffraction peak of 27.4° was also observed, characteristic of the rutile crystalline phase (SHAHVARANFARD *et al.*, 2020) of plane (110). The appearance of characteristic signs of the rutile phase may be related to its greater stability in relation to the anatase phase. The peaks related to TiO_2 have intensities related to the levels used in the systems, with the most intense being the nanocomposites with the highest content of this nanoparticle (1 and 2% m/m). The characteristic graphene peaks are not observed, probably due to the low mass percentage used and/or its dispersion in the TPS matrix due to the interaction of the oxygenated groups with starch and glycerol. In Table 3 it is perceived that there was an important increase in the crystallinity of all prepared nanocomposites, especially in the sample containing 1% TiO_2 . This can be attributed to the nucleating effect of NPs, especially when their distribution is homogeneous in the polymeric matrix, and an important reduction in the size of crystallites, which can be associated with the greater number of crystals formed and the steric hindrance generated by them.

Table 3. Comparative XRD results of samples of mandioca starch, mandioca TPS and TPS/ TiO_2 /graphene nanocomposites

Samples	Crystallinity Degree (%)	Crystallitesize (nm)
Mandioca	30.9	46.2
TPS mandioca	35.0	28.0
TPS 0,5% TiO_2 + 0,1% G	38.7	13.3
TPS 1% TiO_2 + 0,1% G	48.3	15.4
TPS 2% TiO_2 + 0,1% G	39.3	14.4

Determination of the flow index (MFI): The MFI (melt flow index) is used to evaluate the rheological characteristics of the polymer, being important, for example, in the determination of possible processing conditions. Flow index measurements were applied to evaluate the influence of nanoparticles on the viscosity parameters of the prepared materials, an important characteristic for the use of coating materials, whether by spraying or immersion. The evaluation results are presented in Table 4, where it is possible to notice that the nanocomposites suffered a reduction in fluidity compared to pure TPS. The reduction in mass flow rate values (g/10 min) observed for all systems containing nanoparticles indicates an increase in viscosity with the addition of nanoparticles in TPS.

This result can be explained by the fact that the nanoparticles have a high specific area, which favors a strong intermolecular interaction with the polymeric matrix, thus the adsorption of nanoparticles on the starch chains can result in increased viscosity. Another factor that may have added to this change is the increase in the degree of crystallinity. The most recognizable effect on the melt index was noted for the system containing 0.5% m/m of TiO_2 , suggesting a better dispersion of these NPs in the TPS matrix. These interactions increase the resistance to deformation to impede the flow of the polymer in the molten state, hindering or limiting the flow of the polymer in the molten state (CABELLO-ALVARADO, 2019). The absorbance of TiO_2 nanoparticles in the thermoplastic starch matrix, mainly in the length range referring to ultraviolet light, is an important factor to be analyzed due to the fruit ripening processes and also the photo-oxidative process of the polymeric matrix. The absorbance spectra of TPS and TPS/ TiO_2 /graphene nanocomposites are shown in Figure 4.

Ultraviolet-visible absorption spectroscopy (UV-VIS): It was found that pure TPS practically does not absorb ultraviolet radiation. In contrast, the incorporation of TiO_2 NPs into the polymeric matrix

resulted in increased absorption in the ultraviolet A (UV-A) and ultraviolet B (UV-B) regions.

Table 4. Fluidity Index values of TPS/ TiO_2 /graphene nanocomposites compared to cassava TPS

Sample	Mass flow rate(g/10 min)
TPS cassava	4.7
TPS 0,5% TiO_2	3.2
TPS 1% TiO_2 +0,1%G	3.5
TPS 2% TiO_2 +0,1%G	3.9

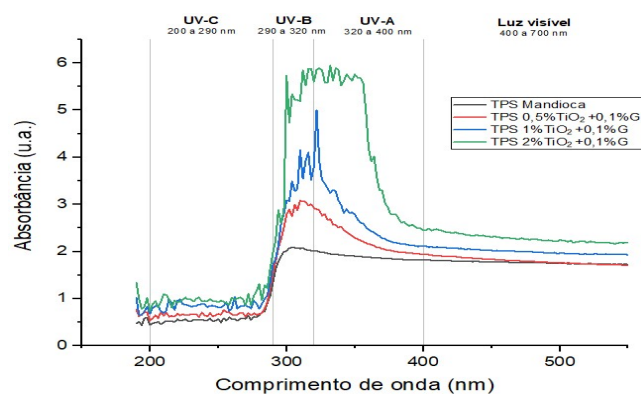


Figure 4. Absorbance spectra of samples in the UV-vis region: cassava TPS and TPS/ TiO_2 /graphene nanocomposites with different contents of nanoparticles

This result was even more expressive with the increase in the content of TiO_2 NPs, as also observed by GOUDARZI, 2017. A higher concentration of NPs in the matrix, once they are well dispersed, offers a greater effective surface area available for absorption ultraviolet. The ability to absorb ultraviolet radiation by TiO_2 NPs can be explained because the band gap energy of this oxide is of the same order of magnitude as the energy of UV radiation, which allows the absorption of this radiation by the electronic structure of TiO_2 (MOHR *et al.*, 2019). It was also observed a displacement of the absorption peaks to the right as the percentage of TiO_2 increases in the system. The highest intensity absorption peak was obtained at 332 nm for the nanocomposite containing 2% m/m of TiO_2 . In addition, through the Planck equation, it was possible to obtain the band gap value of 3.73 eV. This band gap value is within the classification for semiconductors, being higher than the TiO_2 band gap in the anatase phase, which is 3.2 eV (DEL ANGEL *et al.*, 2018). This result can be attributed to the fact that TiO_2 NPs are associated with graphene sheets, which can lead to an improved photocatalytic performance compared to its initial form. Graphene, in turn, has a π conjugation system (electron sharing) and a flat two-dimensional structure, which favors its use as an acceptor and electron carrier (KHOA *et al.*, 2012). Thus, the developed systems have potential for application in biodegradable coatings with UV radiation blocking, which becomes interesting since food exposed to solar radiation suffers acceleration in the deterioration process from photochemical degradation reactions. Besides, the shelf life of foods can also be reduced due to the loss of their organoleptic properties.

Dynamic light scattering (DLS) and zeta potential: The dynamic light scattering technique evaluates the particle size distribution and was used to determine the particle size of TPS and TPS/ TiO_2 /graphene nanocomposites after spray drying. It was seen that the addition of NPs in the TPS matrix interferes with the size distribution of the generated systems. For the lowest concentration of NPs studied (0.5% m/m), a reduction in particle size was observed in relation to pure TPS. However, there is no linear correlation between the NPs content and the size distribution, as can be seen in Table 5. This behavior may be related to the difference in shape and size of the NPs that can be randomly distributed in the TPS matrix, where TiO_2 has a shape close to spherical and graphene has a sheet shape. It is postulated that the relationship between the NPs contents may be

interfering with the distribution of charges in the matrix and the viscosity of the system, changing the size of the system particles observed by the DLS. Another factor that may be interfering with the size assessment of the studied system is the fact that DLS is sensitive to larger-sized macromolecules; amylose and amylopectin contents may offer different contributions to the particle size distribution (Bloomfield, 2002). The analysis of the zeta potential evaluates the sum of system charges and can be correlated with its stability. The greater the value in modulus of the zeta potential, the more stable the system is, since the charged particles repel each other, causing this repulsion to overcome the natural tendency to aggregation. Systems with higher TiO₂ contents (1 and 2% m/m) showed high stability (values greater than 30 mV, GUMUSTAS *et al.*, 2017) being considered the most stable systems among those studied.

Table 5. DLS results of the analyzed solutions of cassava TPS and TPS/TiO₂/graphene nanocomposites

Sample	Diametermedium hydrodynamic (nm)	Potencial zeta (mV)	Polydispersion index
TPS Mandioca	3785	9.58	0.605 ± 0.078
0,5% TiO ₂ + 0,1%G	3140	14.40	0.689 ± 0.033
1% TiO ₂ + 0,1% G	3922	37.20	0.812 ± 0.046
2% TiO ₂ + 0,1% G	3447	38.43	1.548 ± 0.056

Evaluation of the effect of coating fruits in polymeric solution containing TiO₂ and graphene nanoparticles: To evaluate the effect of the TPS/TiO₂/ graphene nanocomposite as a protective coating on the surface of perishable fruits, two coating methods were carried out: by spraying, using Gala apple as test fruit; and by immersion using green apple and guava. To carry out the test, the composition TPS/1%TiO₂/ 0.1% graphene was selected, as it presented greater crystallinity, which is an important characteristic for helping in the barrier property. Aspects such as: degradation time, effect on the color and aesthetics of the fruit, adhesion of the coating on the surface of the fruit and ripening were verified. Figure 5 shows how the polymeric solution spray coating test was performed and how the Gala apples were conditioned.

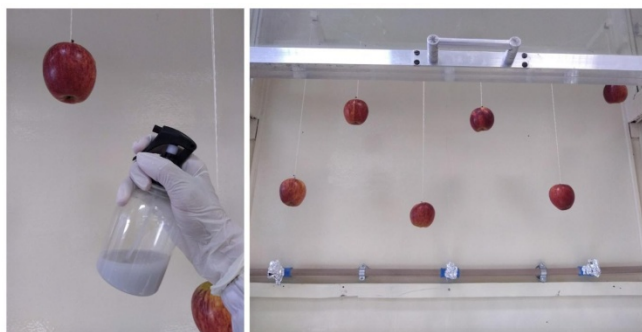


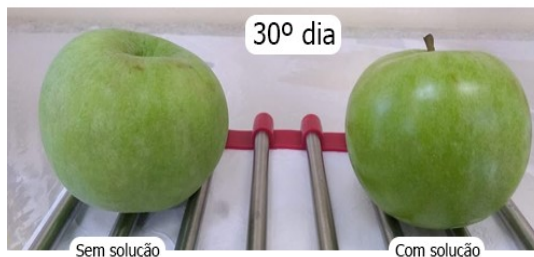
Figure 5. Spray coating test of TPS/1%TiO₂/0.1%graphene polymeric solution on Gala-type apples



Figure 6. Visual comparison over 12 weeks of Gala apples: (a) without application of coating solution and (b) with application of TPS/1%TiO₂/0.1%graphene solution

On average, in up to 24 days, Gala apples presented a consumable visual appearance. Considering the tactile aspect, the Gala apple without solution coating had a “rubbery” consistency, whereas the coated apple had a firm

consistency. After a period of 12 weeks (Figure 6) it was possible to visually observe that for the apples that received coating by spraying the polymeric solution, the degradation process was delayed compared to the process observed for the apples that did not receive the coating, confirming the effect protector of the solution employed.



Figures 7 and 8 show the results obtained for the immersion coating test of green apple and guava fruits, respectively, in a polymeric solution of TPS/1%TiO₂/0.1%graphene.

In Figure 7, the effect of the coating with the polymeric solution on green apples can be seen comparatively. For this fruit, it was possible to analyze the effect on the color and aesthetic perception of the fruit. It was noted that the application of the coating contributed to an improvement in the visual appearance of the fruit, providing a more intense shine, which may be associated with greater protection against UV light. In addition, greater pulp firmness was observed. The fruits without the solution, in general, had a much softer pulp with a “rubbery” touch, while the coated fruits showed greater firmness when handled. This effect was also observed in Gala apples, as discussed earlier. Regarding the visual aspect, for Gala apples it was not possible to observe results as clear as those observed for green apples, due to the surface with a marbled look, characteristic of the green apple itself. However, after 30 days the green apple that was not placed in solution appeared opaquer and duller, and with a rubberier aspect, which was felt by touch. The test carried out for the guava fruit showed advanced ripening for the fruit as early as the seventh day (Fig. 8a), when not immersed in the solution containing the starch and nanoparticles. However, the application of the polymeric solution containing the nanoparticles contributed significantly to delaying the guava ripening process, keeping the fruit completely intact and without signs of decomposition after this period (Fig. 8b).

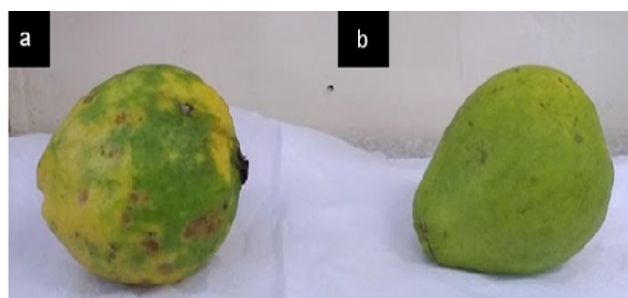


Figure 8. Visual comparison over 7 days for guava: (a) without application of solution and (b) with immersion of TPS/1%TiO₂/0.1%graphene solution

CONCLUSION

Thermoplastic starch (TPS)/TiO₂/graphene nanocomposites were produced from the solution dispersion technique followed by spray drying and subsequently characterized. It was demonstrated that the produced nanocomposites, especially those with 1% (m/m) of TiO₂, showed an increase in crystallinity compared to pure TPS. It was also possible to observe that the materials produced were highly effective in absorbing UV-A and UV-B radiation. The FTIR results suggested a strong interaction between cassava TPS and the used nanoparticles. The nanocomposite solutions showed high dimensional stability, which favored a good dispersion of NPs. Through the coating test on the fruits, it was possible to observe that the applied solution improved its visual characteristics and that it significantly delayed the degradation process of the evaluated fruits. The results indicate that coatings using nanoparticles have great potential to be explored, mainly related to the increase in post-harvest food shelf life and also for long-distance shipping.

REFERENCES

- Forbes Hamish, Queded Tom, O'Connor Clementine. (Food Waste Index Report 2021. United Nations Environment Programme, 2021. Food Waste Index Report 2021). Nairobi.
- UNICEF. The State of Food Security and Nutrition in the World 2021. July 2021 <https://data.unicef.org/resources/sofi-2021/>
- FAO. Reduzir a perda de alimentos e o desperdício ajuda a lidar com as mudanças climáticas. 2019. <https://www.fao.org/brasil/noticias/detail-events/pt/c/1205347/>
- IPEA. Instituto de Pesquisa Econômica Aplicada. Agenda 2030. Objetivos de Desenvolvimento Sustentável. 2018.
- Porpino, G.; Lourenço, C. E.; Araújo, C.M.; Bastos, A.. Intercâmbio Brasil – União Europeia sobre desperdício de alimentos. Relatório final de pesquisa. Brasília: Diálogos Setoriais União Europeia – Brasil, 2018
- Gandra A. Agência Brasil. Pesquisa aponta que fome atinge 33,1 milhões de pessoas no país. 2022.
- UNEP. PNUMA e FAO convocam movimento no Brasil para reduzir perdas e desperdícios de alimentos, 2021.
- Shaikh S., Yaqoob M., Aggarwal P. An overview of biodegradable packaging in food industry. *Current Research in Food Science* 4, 503-520, 2021.
- Velasco, K.E.R., Silva C.A.U., Barrios A.D., Márquez A.E.S, Tafur J.P., Michell R. M. Green Nanocomposites Based on Thermoplastic Starch: A Review. *Polymers*, 13, 3227, 2021
- FLORES, S., FAMÁ, L., ROJAS, A. M., GOYANES, S., & GERSCHENSON, L.; Physical properties of tapioca-starch edible films: Influence of filmmaking and potassium sorbate. *Food Research International*, 40, 257–265, 2007.
- LIM JY, MUBARAK, NM.; ABDULLAH, EC, NIZAMUDDIN, S, KHALID M, INAMUDDIN. Recent trends in the synthesis of graphene and graphene oxidebased nanomaterials for removal of heavy metals — A review. *Journal of Industrial and Engineering Chemistry*, 66, 29–44, 2018.
- MIRANDA, V. R.; CARVALHO, A. JF. Blendas compatíveis de amido termoplástico e polietileno de baixa densidade compatibilizadas com ácido cítrico. *Polímeros*, v. 21, n. 5, p. 353-360, 2011.
- SIWINSKA-CIESIELCZYK, K., SWIGO'N, D., RYCHTOWSKI, P., MOSZYŃSKI, D., ZGOŁA-GRZE' SKOWIAK, A., JESIONOWSKI, T., The performance of multicomponent oxide systems based on TiO₂, ZrO₂ and SiO₂ in the photocatalytic degradation of rhodamine B: mechanism and kinetic studies. *Colloids Surf. A Physicochem. Eng. Asp.* 586, 124272, 2020
- CABELLO-ALVARADO, C. et al. Melt-mixed thermoplastic nanocomposite containing carbon nanotubes and titanium dioxide for flame retardancy applications. *Polymers*, 11, 1204, 2019.
- CHEN, H.; XIE F.; CHEN L.; ZHENG, B.; Effect of rheological properties of potato, rice and corn starches on their hot-extrusion 3D printing behaviors. *Journal of Food Engineering*, 244, 1 50-158, 2019.
- ÇIPLAK, Z.; YILDIZ, N.; ÇALIMLI, A. Investigation of graphene/Ag nanocomposites synthesis parameters for two different synthesis methods. *Fullerenes, Nanotubes and Carbon Nanostructures*, 23, 361-370, 2014
- Zielinska D, Siwinska-Ciesielczyk K, Bula Karol, Jesionowski T, Borysiak S., TiO₂/nanocellulose hybrids as functional additives for advanced polypropylene nanocomposites. *Ind. Crops Prod.*, 2022
- LOUDARZI, V., SHAHABI-GHAHFARROKHI, I., & BABAEI-GHAZVINI, A. Preparation of ecofriendly UV-protective food packaging material by starch/TiO₂ bio-nanocomposite: Characterization. *International Journal of Biological Macromolecules*, 95, 306–313, 2017.
- MOHR, L. C.; CAPELEZZO, A. P.; BARETTA, C. R. D. M.; MARTINS, M. A. P. M.; FIORI, M. A.; MELLO, J. M. M. Titanium dioxide nanoparticles applied as ultraviolet radiation blocker in the polylactic acid biodegradable polymer. *Polymer Testing*, 77, 105867, 2019.
- DEL ANGEL, R.; DURÁN-ÁLVAREZ, J. C.; ZANELLA, R. TiO₂-Low Band Gap Semiconductor Heterostructures for Water Treatment Using Sunlight-Driven Photocatalysis. In: *Titanium Dioxide-Material for a Sustainable Environment*. Intech Open, 2018.
- KHOA, N. T.; PYUN, M. W.; YOO, D. H.; KIM, S. W.; LEEM, J. Y.; KIM, E. J.; HAHN, S. H. Photodecomposition effects of graphene oxide coated on TiO₂ thin film prepared by electron-beam evaporation method. *Thin Solid Films*, 520, 5417-5420, 2012.
- VAN SOEST, J. J. G & Vliegenthart, J. F. G., Crystallinity in starch plastics: consequences for material properties, *Trends in Biotechnology*, 15, 208, 1997.
- Hernandez JHM., Effect of the Incorporation of Polycaprolactone (PCL) on the Retrogradation of Binary Blends with Cassava Thermoplastic Starch (TPS). *Polym.* 13, 38, 2021
- Van Soest JJG, Hulleman SHD, Vit D, Vliegenthart JFG., Crystallinity in starch bioplastics. *Ind. Crop. Prod.* 5, 11, 1996
- Thajai N, Jantanasakulwong K, Rachtanapun P, Jantrawut P, Kiattipornpithak K, Kanthiya T, Punyodom W., Effect of chlorhexidine gluconate on mechanical and anti-microbial properties of thermoplastic cassava starch. *Carbohydr. Polym.* 275, 118690, 2022
- Ostafińska A, Mikešová J, Krejčíková S, Nevalová M, Štuncová A, Zhigunov A, Michálková D, Šlouf M., Thermoplastic starch composites with TiO₂ particles: Preparation, morphology, rheology and mechanical properties. *Int. J. Biol. Macromol.* 101, 273-282, 2017
- ÇIPLAK, Z.; YILDIZ, N.; ÇALIMLI, A. Investigation of graphene/Ag nanocomposites synthesis parameters for two different synthesis methods. *Fullerenes, Nanotubes and Carbon Nanostructures*, v. 23, n. 4, p. 361-370, 2015.
- Thamaphat K., PichetLimsuwan, BoonlaerNgotawornchai Phase Characterization of TiO₂ Powder by XRD and TEM. (*Nat. Sci.*) 42, 357 – 361, 2008
- Pascal Voepel, Morten Weiss, Bernd M. Smarsly, Roland Marschall. Photocatalytic activity of multiphase TiO₂(B)/anatase nanoparticle heterojunctions prepared from ionic liquids. *Journal of Photochemistry and Photobiology A: Chemistry*. 366, 34-40, 2018,